JOURNAL OF MATERIALS SCIENCE 25 (1990) 4567–4570

Microstructural development in non-oriented lamination steels

Part III *The observation of cavities in the temper-rolled condition*

J-W. LEE*, P. R. HOWELL
Department of Materials Science and Engineering, The Pennsylvania State University, University Park, Pennsylvania 16802, USA

Two low carbon steels, in the temper-rolled condition, have been examined using a combination of light microscopy, scanning electron microscopy and transmission electron microscopy. The thermomechanical processing fragments the pearlite colonies and both cavities and cracks were found to be associated with cementite particles. It is suggested that these cracks and cavities arise during cold rolling due to the interaction of dislocation pile-ups with cementite. Subsequent growth occurred during continuous annealing.

1. Introduction

The increasingly strict requirement of superior magnetic properties on electrical steels necessitates detailed microstructural investigations in that the electrical losses are closely associated with microstructural factors. It is thus highly likely that guidance in developing better materials can be provided by a fundamental understanding of the microstructural changes accompanying processing. Recent proceedings of conferences on "Energy Efficient Electrical Steels" [1] and the 1985 "Symposium on the Physical Metallurgy of Electrical Steels" [2] have shown a growing awareness of the importance of studying those microstructural details which are associated with energy losses.

In practical engineering situations, low carbon steels are often used as electrical steels in a laminated form, however, prior to usage as electromagnetic devices, these steels undergo severe cold rolling to develop the required texture, followed by continuous annealing and temper rolling. Finally, the temper rolled materials are decarburized in the two-phase ferrite–austenite region. Little information is available in the literature concerning the microstructural development of lamination steels during processing and the available data pertain generally to the microstructures of the steels after decarburization, hence, as a part of a detailed examination of the microstructures of lamination steels, two such steels have been examined in the temper rolled condition.

2. Experimental procedures

The investigation was conducted on temper rolled (0.50 mm thick) steels which were obtained from Inland Steel, Chicago, Illinois. The chemical compositions of these steels are presented in Table I. The processing schedule of these steels is shown in Fig. 1 of Lee and Howell [3]. The steels underwent $\sim 70\%$ cold rolling followed by continuous annealing (at $\simeq 720°$ C) and then a 4 to 6% temper roll.

Light microscopy, scanning electron microscopy (SEM) and transmission electron microscopy (TEM) techniques have been employed for microstructural examination. Specimens for light microscopy and SEM were mechanically polished and etched in 2% nital. SEM examinations were conducted on an ISI Super IIIA using an accelerating potential of 25 kV. Specimens for TEM were prepared in a twin-jet electropolisher using an electrolyte consisting of 5% perchloric acid in glacial acid at room temperature and at a potential of 35 V. TEM investigations were performed on a Philips EM 300 operating at 100 kV.

3. Results

Prior to rolling and annealing, the microstructures of the two steels comprised:

(i) an equiaxed ferrite grain structure;
(ii) isolated islands of pearlite;
(iii) massive films of cementite, both at ferrite grain boundaries and at ferrite–pearlite interfaces†.

Fig. 1 is a light micrograph of temper rolled steel A. In essence, the thermomechanical treatment of these two steels leads to:

(1) an equiaxed ferrite grain structure (mean grain size $\simeq 30\,\mu$m): and
(2) a fragmented cementite distribution.

The cementite precipitates are often associated with ferrite grain boundaries (arrowed A on Fig. 1) but can also occur intragranularly (arrowed B on Fig. 1). In addition, the pearlitic colonies observed in the hot

*Present address: Department of Metallurgical Engineering and Materials Science, Carnegie–Mellon University, Pennsylvania 15213, USA.
†Further details on the microstructures of the "as-received" materials are given in [3].

TABLE I Alloy compositions (wt %)

	C	Mn	Si	P	S	Al	N
Temper rolled steel A	0.04	0.5	0.04	0.13	0.02	–	0.006
Temper rolled steel B	0.04	0.25	0.20	0.09	0.02	0.25	0.006

rolled condition are fragmented. These fragmented colonies (arrowed C) are elongated along the rolling direction.

Figs 2 to 5 (from steel A) are SEM micrographs from areas containing significant amounts of cementite*. From Figs 2 to 5 it can be seen that

(1) the massive films of cementite and the majority of the pearlitic regions observed in the hot rolled steels have been fragmented by subsequent thermomechanical treatment; and

(2) numerous cavities are observed.

The smaller and discrete cementite precipitates, however, often do not show any evidence for cracking or cavitation during thermomechanical treatment as shown in Fig. 5 (arrowed). In Figs 2 to 4, cavities are associated with cementite–ferrite interfaces (arrowed A and B). This observation suggests that the cavities form invariably at the cementite–ferrite interfaces. The shape of the cavities is approximately spherical. Similarly, the cementite which is associated with the fragmented pearlite colonies is often non-lamellar in shape (Fig. 2). In addition to cavitation, evidence for cracks in the cementite was observed (arrowed C in Fig. 3). Some of the pearlite colonies still exhibited an approximately lamellar morphology even after thermomechanical processing as shown in Fig. 4. In this instance, a cavity is observed at a ferrite–cementite interface within the pearlite colony.

Figs 6 and 7 are typical TEM micrographs of the temper rolled steels. Evidence for the formation of dislocation cells is apparent in Fig. 6, whilst the massive film of cementite in Fig. 7 exhibits brittle cracking (arrowed). These cracks have not, however, developed into cavities. Basically, three types of crack have been observed. The cementite film shown in Fig. 8 exhibits shear cracking as evidenced by the offsets in the film (arrowed). In Fig. 9, the cementite film has been partially necked down (arrowed). This necking is clear evidence for plastic deformation of the cementite.

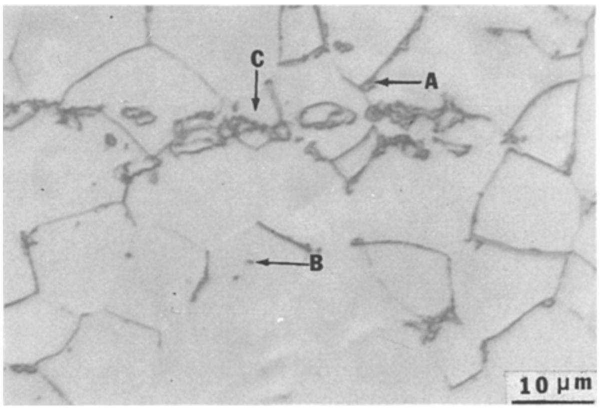

Figure 1 Light micrograph of temper rolled steel A showing equiaxed ferrite and fragmented pearlite colonies.

*Similar results were obtained for steel B.

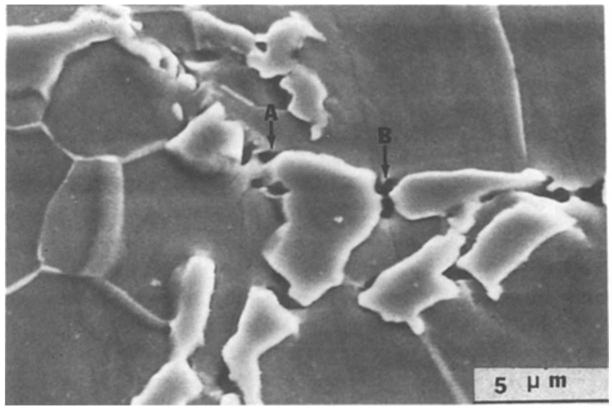

Figure 2 SEM micrograph of temper rolled steel A showing that numerous cavities are associated with large cementite particles.

Finally, Fig. 10 shows a small cementite precipitate which had not initiated cracking.

4. Discussion

Although cavitation in low alloy steels is not uncommon, to the authors' knowledge, cracking and cavitation have not been reported previously in processed lamination steels. It is, however, known [4, 5] that pre-strain at room temperature accelerates cavitation in certain nickel-base alloys by the interaction of dislocation pile-ups with hard carbide particles at grain boundaries. In the present case, it would appear that many of the cavities grow under the driving force of pre-strain at the continuous annealing stage, but are caused by the interaction of dislocation flow with cementite during cold rolling.

In the steels investigated, it is suggested that dislocations pile up at ferrite–cementite interfaces during rolling, thereby creating a stress concentration. If the cohesive strength of the cementite–ferrite interface is less than the stress at the head of the pile-up, cracking can occur at the interface between ferrite and cementite and the crack will propagate into the cementite. The thickness of the cementite films is, however, also an important factor since Miller and Pilkington [6] observed that cavities in low alloy steels nucleate at larger carbide particles on grain boundaries but not at small particles when deformed at high temperature.

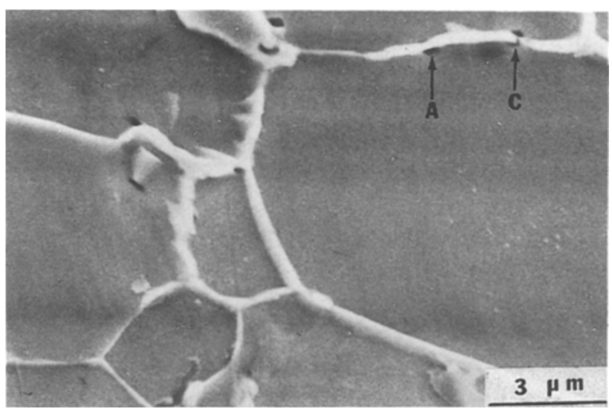

Figure 3 SEM micrograph of temper rolled steel A revealing cavities and cracks in association with the grain boundary precipitates of cementite.

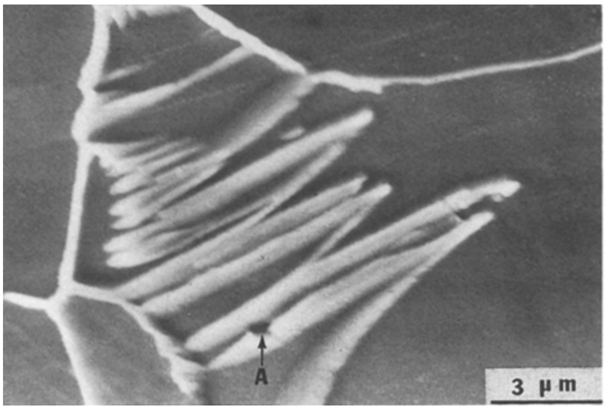

Figure 4 SEM micrograph of temper rolled steel A showing cavities at pearlitic ferrite–cementite lamellae interfaces.

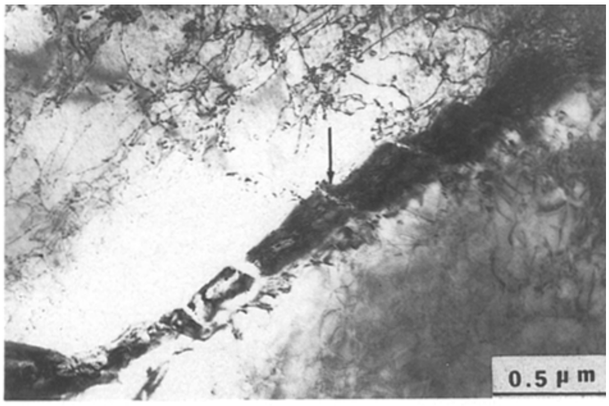

Figure 8 Thin-foil micrograph of temper rolled steel B showing shear cracking of the cementite film.

The reason why small particles do not crack is that the stress concentration required to initiate cracking cannot be achieved, instead, local plastic deformation occurs. This is consistent with the present findings where the propensity for cracking decreased as the particle size decreased.

As indicated by other investigations [4, 5], cracking can develop into cavities at high temperature by the diffusional transfer of the excess vacancies which were created by the cold rolling. The driving force is, however, provided by pre-strains. The exact stage at which the cracks develop into cavities is uncertain. For example, during recovery (which often precedes recrystallization [7]), dislocations and sub-boundaries could provide effective diffusion paths for excess vacancies. In addition, it is known [8] that recrystallization is completed during the anneal and the cavities could coarsen at the recrystallization interface. Similarly, it has been established that for these steels, partial reaustenitization occurs after 60 sec at 720° C [9]. Again, the passage of e.g., a pearlite–austenite interface can lead to either the formation of cavities from the cracks or coarsening of pre-existing cavities. It is also expected that the final temper rolling would also lead to the development of new cracks and cavities in addition to promoting further growth of pre-existing cracks. It is beyond the scope of this study to comment in detail on specific mechanisms of the nucleation and growth of cavities. Detailed work on these mechanisms will be presented elsewhere [8].

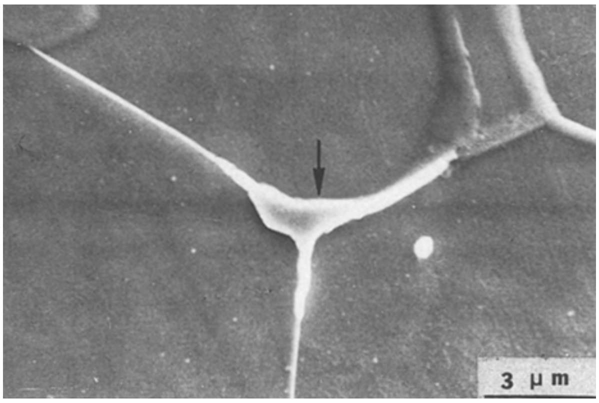

Figure 5 SEM micrograph of temper rolled steel A showing no cracks at thin grain boundary films of cementite.

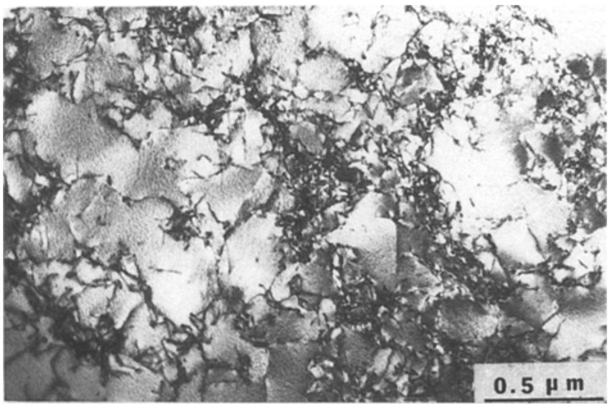

Figure 6 Thin-foil micrograph of temper rolled steel B illustrating the formation of dislocation cells.

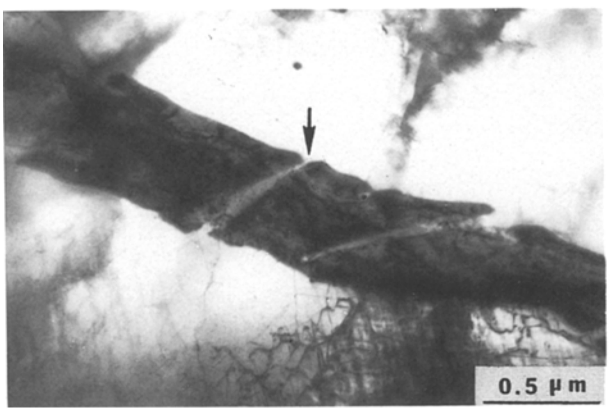

Figure 7 Thin-foil micrograph of temper rolled steel B. Note cracks in the cementite film.

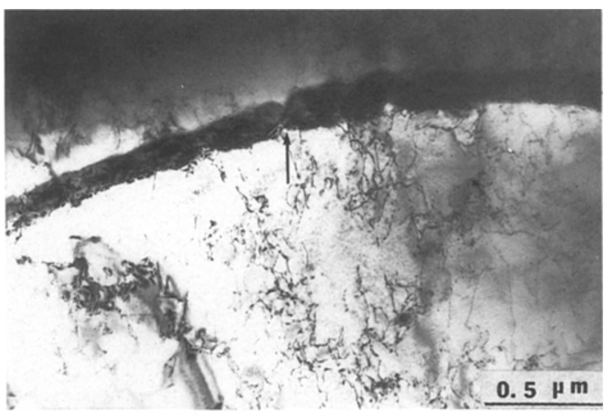

Figure 9 Thin-foil micrograph of temper rolled steel B. Note necking down of the cementite film.

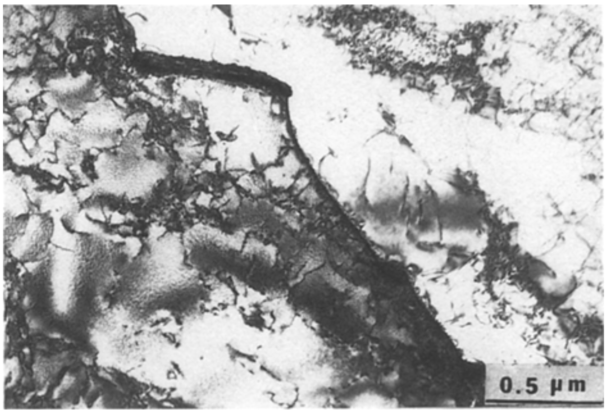

Figure 10 Thin-foil image of temper rolled steel B showing no cracking of the small, discrete cementite precipitates.

The morphology of the fragmented pearlite colonies created by prior cold rolling can be changed from that observed in the hot rolled conditions during subsequently continuous annealing since the continuous annealing leads to recrystallization of the deformed ferrite and partial reaustenitization. From reaustenitization studies on cold rolled specimens, it was found [8, 9] that partial reaustenitization had occurred and recrystallization was complete within this period. Hence, it is suggested that during continuous annealing, the cementite lamellae in those fragmented colonies which are not consumed by austenite, spheroidize during recovery–recrystallization. Conversely, those colonies which do transform to austenite can revert to a lamellar pearlitic structure during cooling from the continuous anneal. The above could explain the dissimilar carbide distributions observed in Figs 2 and 4.

5. Conclusions

From the results of the present investigation, the following conclusions can be drawn.

(1) The temper rolled materials consisted of

(a) equiaxed ferrite grains,

(b) intergranular and intragranular cementite precipitates,

(c) fragmented pearlite colonies.

(2) Cavities which were associated with cementite were found. These cavities most probably arose due to the interaction of dislocation pile-ups with cementite during cold rolling. Growth is postulated to occur by the short-circuit diffusion of excess vacancies during continuous annealing.

Acknowledgements

The authors are grateful to the American Iron and Steel Institute for financial support. Dr G. Ludkovsky is thanked for providing the specimen materials.

References

1. A. R. MARDER and E. T. STEPHENSON (eds), "Energy Efficient Electrical Steels", (TMS-AIME, Warrendale, Pennsylvania, 1981).
2. Symposium on the Physical Metallurgy of Electrical Steels. *Met. Trans.* **17A** (1986) 1259.
3. J-W. LEE and P. R. HOWELL, *J. Mater. Sci.* **22** (1987) 3631.
4. B. F. DYSON and D. E. HENN, *J. Microsc.* **97** (1973) 165.
5. T. SAEGUSA, M. UMERA and J. R. WEERTMAN, *Met. Trans.* **11A** (1980) 1453.
6. D. A. MILLER and R. PILKINGTON, *ibid.* **9A** (1978) 489.
7. P. GORDON, *Trans. Met. Soc. AIME* **203** (1955) 1043.
8. J-W. LEE and P. R. HOWELL, *J. Mater. Sci.* submitted.
9. *Idem, J. Mater. Sci.* to be submitted.

Received 19 June
and accepted 22 November 1989